Mechanism of Formation of Novel Covalent Drug·DNA Interstrand Cross-Links and Monoadducts by Enediyne Antitumor Antibiotics[†]

Yong-jie Xu,[‡,§] Zhen Xi,[‡] Yong-su Zhen,[§] and Irving H. Goldberg*[,‡]

Department of Biological Chemistry and Molecular Pharmacology, Harvard Medical School, 250 Longwood Avenue, Boston, Massachusetts 02115, and Institute of Medicinal Biotechnology, Chinese Academy of Medical Sciences, Tiantan, Beijing 100050, China

Received August 25, 1997; Revised Manuscript Received September 26, 1997[⊗]

ABSTRACT: The potent enediyne antitumor antibiotic C1027 has been previously reported to induce novel DNA interstrand cross-links and drug monoadducts under anaerobic conditions [Xu et al. (1997) *J. Am. Chem. Soc. 119*, 1133−1134]. In the present study, we explored the mechanism of formation of these anaerobic DNA lesions. We found that, similar to the aerobic reaction, the diradical species of the activated drug initiates anaerobic DNA damage by abstracting hydrogen atoms from the C4′, C1′, and C5′ positions of the A1, A2, and A3 nucleotides, respectively, in the most preferred 5′GTTA1T/5′ATA2A3C binding sequence. It is proposed that the newly generated deoxyribosyl radicals, which cannot undergo oxidation, likely add back onto the nearby unsaturated ring system of the postactivated enediyne core, inducing the formation of interstrand cross-links, connecting either A1 to A2 or A1 to A3, or drug monoadducts mainly on A2 or A3. Comparative studies with other enediynes, such as neocarzinostatin and calicheamicin γ_1^I under similar reaction conditions indicate that the anaerobic reaction process is a kinetically competitive one, depending on the proximity of the drug unsaturated ring system or dioxygen to the sugar radicals and their quenching by other hydrogen sources such as solvent or thiols. It was found that C1027 mainly generates interstrand cross-links, whereas most of the anaerobic lesions produced by neocarzinostatin are drug monoadducts. Calicheamicin γ_1^I was found to be less efficient in producing both lesions. The anaerobic DNA lesions induced by enediyne antitumor antibiotics may have important implications for their potent cytotoxicity in the central regions of large tumors, where relative anaerobic conditions prevail.

The extreme potencies of the enediyne antitumor antibiotics, such as the calicheamicins, esperamicins, C1027, and neocarzinostatin (Figure 1), are believed to be due to their ability to induce single-strand (SS) or double-strand (DS) damage in cellular DNA (*1*). These agents can be activated by reducing compounds or a spontaneous process to form a diradical species that interacts with DNA in the minor groove and abstracts hydrogen atoms from minor-groove-accessible carbons of the sugar backbone of each complementary DNA strand. So far, three main attack sites (C5′, C4′, and C1′) and the resulting damage products, which include abasic sites and strand breaks, have been characterized (Figure 2). Most of the previously reported DNA damage induced by enediynes was studied, however, in the presence of molecular oxygen (*1*). In cancer chemotherapy, the relative hypoxic conditions in the centers of solid tumors might influence the DNA damage pathway, causing different lesions and hence modifying the chemotherapeutic efficiency of these antibiotics. Indeed, we have recently shown that when O_2 was depleted from drug/DNA reaction systems, enediyne C1027 induces the formation of novel interstrand cross-links and drug monoadducts, instead of strand breaks and abasic lesions (*2*). Some earlier studies with neocarzinostatin have also demonstrated that this agent produces drug monoadducts under anaerobic conditions (*3*) and that adduction is on the deoxyribose of the attacked nucleotide target (*4*, *5*).

In the present study, the mechanism by which C1027 produces interstrand cross-links and drug monoadducts was investigated. We found that by using DNA oligomers with the target 5′GTTA1T/5′ATA2A3C sequence (damaged residues are numbered), where C4′-, C1′-, and C5′-hydrogens at A1, A2, and A3, respectively, are abstracted by the drug diradical, interstrand cross-links are formed by the drug itself connecting either A1 and A2 or A1 and A3. Observation of an isotope selection effect by position-specific deuteriation at the C1′ position of A2 and other experiments strongly indicate that position-specific hydrogen abstraction by the activated drug (Figure 1) from DNA deoxyribose is a key step in initiating the process of cross-linking and adduction. To compare different drug/DNA reaction systems, other enediynes, such as neocarzinostatin and calicheamicin γ_1^I, were also tried under similar anaerobic reaction conditions. In contrast, neocarzinostatin and calicheamicin γ_1^I mainly produce drug monoadducts, and their yields depend on the concentrations and the types of thiols and solvents used in the reaction systems. Quantitation of the aerobic and anaerobic damage products in different drug/DNA reaction systems implies that accessibility of O_2 and/or hydrogen sources from solvents and proximity of drug to the DNA sugar radicals in the drug/DNA complexes are important factors determining what types of damage products are

[†] This work was supported by Grant GM 53793 from the National Institutes of Health.

* To whom correspondence should be addressed.

[‡] Harvard Medical School.

[§] Chinese Academy of Medical Sciences.

[⊗] Abstract published in *Advance ACS Abstracts,* November 15, 1997.

S0006-2960(97)02101-6 CCC: $14.00

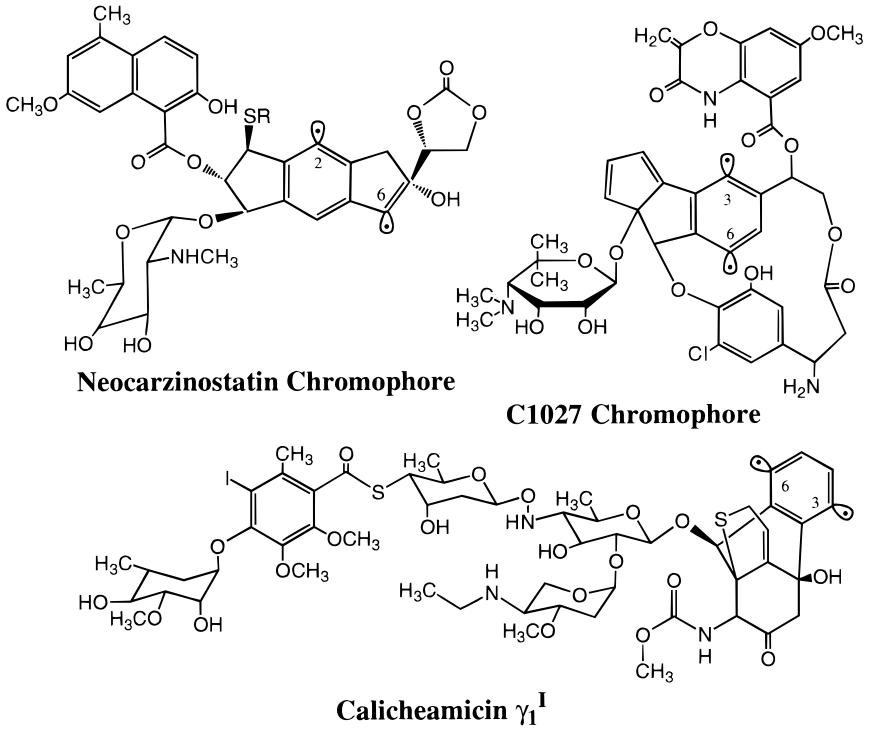

FIGURE 1: Diradical forms of enediyne neocarzinostatin chromophore, C1027 chromophore, and calicheamicin γ_1^I.

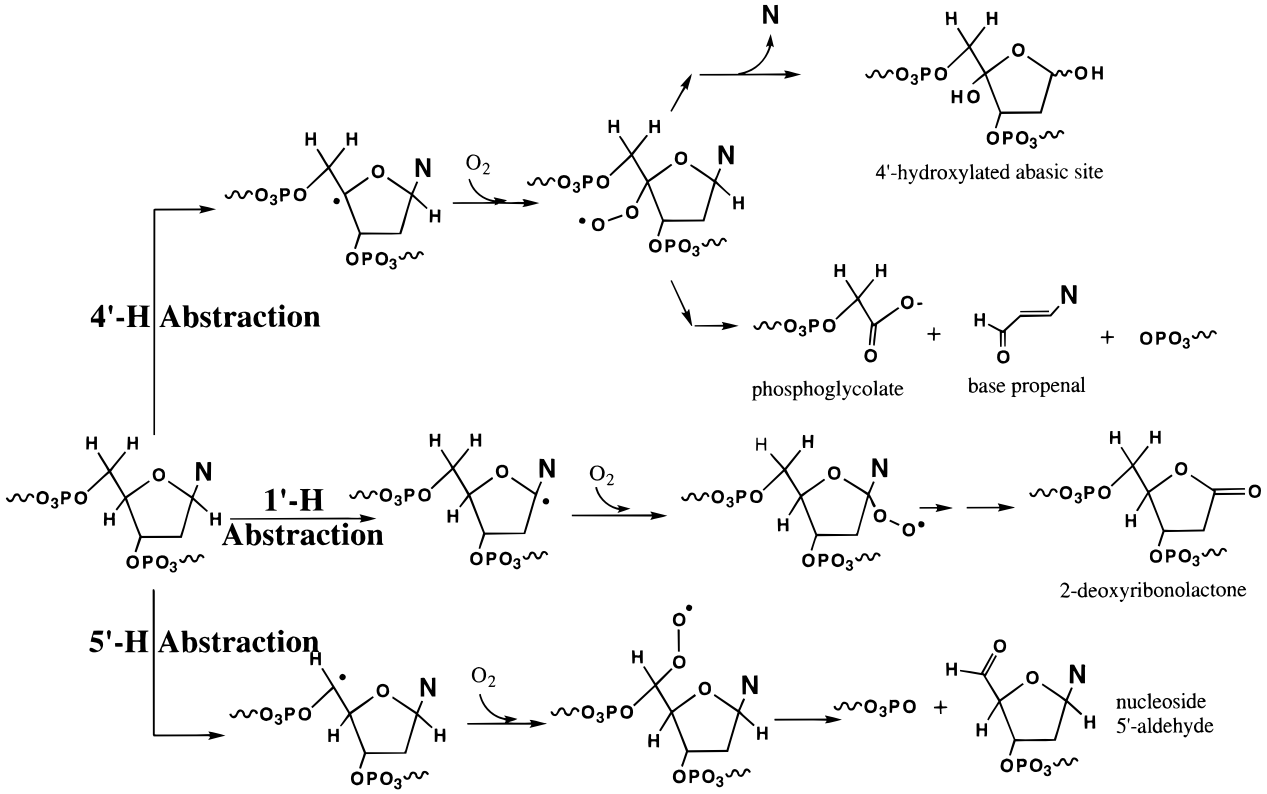

FIGURE 2: Proposed mechanisms for enediyne-induced DNA damage by C4′-, C5′-, and C1′-hydrogen abstractions.

produced. Unlike alkylating agents, whose cross-links involve bases, C1027 induces interstrand cross-links by the drug itself most likely connecting the complementary DNA sugar backbones. These findings have significant implications for not only the nature of interactions between the activated enediyne molecules with DNA targets but also for the remarkable therapeutic effects of this class of antibiotics against solid tumors.

MATERIALS AND METHODS

Materials. Materials and their sources are as follows: holoantibiotic C1027, purified from the fermentation broth of the producing *Streptomyces globisporus* C1027 strain as reported (*6*−*8*); neocarzinostatin and calicheamicin γ_1^I, Kayaku Antibiotics and Dr. George Ellestad of Wyeth-Ayerst Research, respectively; [γ-^{32}P]ATP, New England Nuclear

C1027:

D1 5′-GCC**GTTA$_1$T**GCCG
D2 3′-CGG**CA$_3$A$_2$TA**CGGC

D3 5′-TCG**GTTA$_1$T**CA X
GC**CA$_3$A$_2$TA**GT

Neocarzinostatin:

D4 5′-CGGC**AGC$_1$**GGC
D5 3′-TTGCCG**T$_2$CG**CCGT

D6 5′-CGGC**AGT$_1$**GGC
D7 3′-TTGCCG**T$_2$CA**CCGT

Calicheamicin:

D8 5′-GCCGA**TC$_1$CT**ACG
D9 3′-CGGC$_2$T**AGGA**TGC

D10 5′-AAGCCGA**TC$_1$CT**ACGAC
D11 3′-TTCGGC$_2$T**AGGA**TGC

FIGURE 3: Sequences of oligodeoxyribonucleotide substrates for enediyne antibiotics. Drug interaction sequences are printed in boldface type. D3 is a hairpin oligomer with a hexaethylene glycol group, X, which holds the positive and the negative strands together via two phosphodiesters.

DuPont; T4 polynucleotide kinase and the Klenow fragment of DNA polymerase I, New England Biolabs; phosphoramidites and chemicals for DNA synthesizer, Glen Research; solutions for making sequencing gels, National Diagnostic; other chemical reagents were from Sigma and Aldrich.

Fluorescence. Florescence measurements were performed on a Perkin-Elmer LS 50 B Luminescence Spectrometer. Excitation was at 340 nm, and the emission spectrum was recorded from 370 to 600 nm.

Synthesis and Labeling of Oligodeoxyribonucleotides. All oligodeoxyribonucleotides were synthesized on an Applied Biosystems 381A automatic synthesizer by the phosphoramidite method. Synthesis of 5′-(dimethoxytrityl)-1′-deuteriumyl-2′-deoxy-3′-(cyanoethyl)adenosine phosphoramidite was as previously described (*9*). The specific nucleotide containing the C1′ deuterium label was incorporated manually into the oligomers using standard phosphoramidite methodology. The triethylene glycol chemical linker joining the 5′-end of the positive strand and the 3′-end of the complementary strand via two phosphodiester bonds (D3 in Figure 3) was also incorporated manually. The concentrations of single-strand oligomers were determined by UV absorbance at 260 nm. The 5′-ends of oligomers were labeled with ^{32}P by T4 polynucleotide kinase, and the 3′-ends were ^{32}P labeled by the Klenow fragment of DNA polymerase I. Labeled oligomers were purified by electrophoresis on 20% polyacrylmide gels containing 8.3 M urea.

DNA/Drug Reaction. The end-labeled oligomers were annealed to their complementary strands at the ratio of 1:1.5 by heating at 90 °C for 5 min and slowly cooling to room temperature. A standard reaction mixture contained 10 mM Tris·HCl (pH 8.0), 0.5 mM EDTA, and 10 μM oligomers. To initiate the DNA/drug reactions, holo C1027 (50 μM), holo neocarzinostatin (40 μM), and calicheamicin γ_1^I (15 μM) were separately added to their reaction mixtures. The reactions were usually allowed to proceed in the dark at 37 °C for 3 h or at room temperature overnight and stopped by drying in a Speed-Vac concentrator. Alkaline treatment involved heating one of the duplicate aliquots in 50 μL of 1 M piperidine at 90 °C for 30 min. As for hydrazine and putrescine treatments, either agent was added to a final concentration of 100 mM, and the mixtures were incubated at room temperature or 37 °C, respectively, for 1 h.

The anaerobic reactions were performed in a Warburg vessel. The side arm contained drug (or thiols in the reactions with neocarzinostatin and calicheamicin γ_1^I), and the rest of the components of the reaction mixture were placed in the main chamber. The contents of the flask were frozen in liquid nitrogen and then evacuated at $<10^{-3}$ Torr in a Kontes high-vacuum setup. The freeze−evacuate−thaw procedure was repeated five times, and the vessel was then filled with ultrapure argon (O_2 < 1.0 ppm, Medical Technical Gases, Inc.). After the contents of the two chambers were mixed, the reaction was allowed to proceed in the dark at 37 °C for 3 h or overnight at room temperature. Misonidazole (18.2 mM), when present, was added to the main chamber. To compare with anaerobic reactions, aerobic reactions were similarly treated, but at the end of evacuation the flask was opened and the reaction mixture was exposed to the air.

Analysis of DNA Damage Products by Gel Electrophoresis. The final dried sample pellets were redissolved in 80% (v/v) formamide, containing 1 mM EDTA and marker dyes, and electrophoresed on a 20% sequencing polyacrylmide gel. The gel band intensities were quantitated by scanning with a Molecular Dynamics PhosphorImager instrument, and the data were analyzed by performing volume integration using Image Quant software.

HPLC Separation of DNA Damage Products. The DNA/drug reaction samples were first separated on a 20% sequencing gel. The bands containing cross-linked DNA and monoadducts were visualized by autoradiography and UV shadowing and excised from the gels. The damage products were eluted from the gel slices by using the crush and soak procedure. The supernatant containing eluted samples was then subjected to HPLC purification on a reverse-phase C-18 column using Waters 510 pumps and UV (Type 486) and fluorescence (Type 474) detectors. The HPLC purification was accomplished by using a linear gradient of 7−17% of acetonitrile in 10 mM triethylamine acetate, pH 7.0, over a period of 37 min. The elution was monitored by following 260 nm UV absorbance and 435 nm fluorescence excited at 350 nm, which detects the postactivated C1027.

DNA Sequence Random Fragmentation. Iron(II) EDTA cleavage of DNA was generally performed as described (*10*) with slight modifications. To the DNA solutions containing 10 mM Tris (pH 7.5) was added 1 μL each of 0.2 M ascorbic acid, 3.0% aqueous H_2O_2, and 20 mM $(NH_4)_2Fe(SO_4)_2$. After 2 min incubation at room temperature, the cleavage reaction was stopped by the addition of 2 μL of 0.5 M aqueous thiourea. Samples were then desalted by elution through a Waters Sep-Pak C18 cartridges, dried, and analyzed on a sequencing gel.

RESULTS

Primary Evidence of Covalent Binding of C1027 to DNA. The post-activated C1027 chromophore can bind reversibly to DNA, and the drug/DNA complex is completely dissociated by ethanol precipitation of the DNA (data not shown).

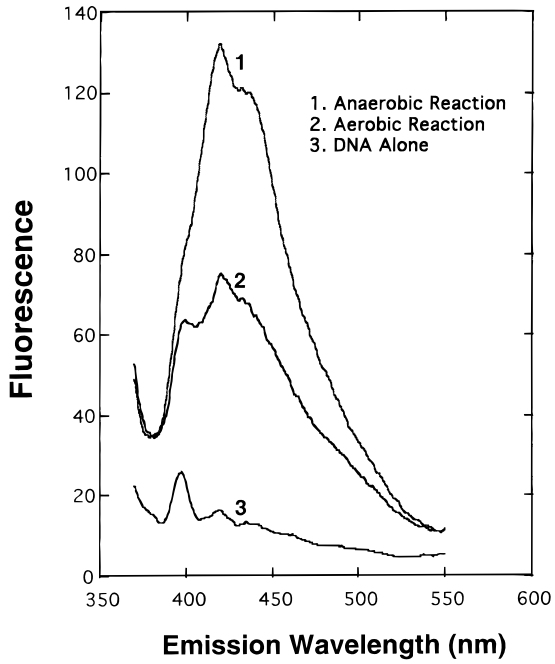

FIGURE 4: Binding of C1027 chromophore to DNA. Calf thymus DNA was incubated with C1027 at 37 °C for 3 h under anaerobic conditions (spectrum 1). C1027 apoprotein was removed by phenol/$CHCl_3$ extractions. The DNA was then precipitated with ethanol (75%) in 0.3 M sodium acetate, pelleted, rinsed twice with 75% ethanol, and dissolved in 20 mM Tris·HCl, pH 8.0, and its fluorescence spectrum was recorded (excitation, 350 nm). The DNA in spectrum 2 was treated identically, except the incubation was done in open air. Spectrum 3, DNA alone.

However, when calf thymus DNA was treated with C1027 under anaerobic conditions, the 435 nm fluorescence attributable to the C1027 chromophore excited at 350 nm (*11*) remains associated with the precipitated DNA. Ethyl acetate, phenol, and chloroform extractions and ethanol precipitations failed to dissociate the DNA/C1027 complex (Figure 4). This preliminary fluorescence experiment suggested that a covalent linkage of C1027 chromophore with DNA might be formed under anaerobic conditions and to a lesser extent under aerobic reactions.

Interstrand Cross-Link and Drug Monoadduct Formation. To further characterize the possible covalent linkage of C1027 with DNA, two complementary DNA oligomers, D1 and D2, containing the most preferred target site 5′GTTA1T/5′ATA2A3C (*12*) were synthesized and 5′-end-labeled, and the anaerobic damage products were analyzed on a high-resolution denaturing gel. Previous studies demonstrated that, at the 5′GTTA1T/5′ATA2A3C sequence, C1027 induces two DS lesions involving either A1 and A2 or A1 and A3 (*9*). The damage, including strand breaks and abasic lesions, are caused by hydrogen abstraction from the C4′ position of A1, C1′ of A2, and C5′ of A3. As shown in Figure 5, under aerobic conditions, damage at A1 affords almost exclusively a 3′-phosphoglycolate fragment, which typically runs slightly faster than the Maxam−Gilbert 3′-phosphate-ended markers (lanes 3−8, indicated by arrow). The slow moving bands, designated by a, b, and c in lane 3, likely represent degradation products of the 4′-hydroxylated abasic lesion at A1 site under the described reaction conditions. Treatment with hydrazine generated a slower moving band of the 3′-phosphopyridazine derivative due to adduct formation with the 4′-hydroxylated abasic lesion (lane 4, designated by asterisk) (*13*). However, when the oligomer D1 duplexed with D2 was treated with C1027 under anaerobic conditions, the cleavage at the A1 site was markedly inhibited (compare lanes 5 and 6 with lanes 3 and 4) and two new sets of bands with slower mobility than the starting substrate D1 were generated (lanes 5 and 6).

On the basis of our previous report (*9*), in the presence of oxygen, the lesion produced at A3 is due to C5′-hydrogen abstraction, and a strand break with a 3′-phosphate was generated (lane 11). The damage at A2 is caused by C1′-attack and a ribonolactone abasic site was formed, which broke down during incubation and later workup. The slowly moving band designated by *d* is an unknown product and probably represents a degraded product of the abasic lesions at A2 sites. In contrast to the damage generated on the D1 oligomer, a slowly moving band denoted by "adduct" (lanes 11 and 12) was generated even under aerobic conditions. Because oligo D2 was well separated from strand D1 on the denaturing gel and these products were only found on strand D2, they most likely represent drug monoadducts attached on the D2 strand. In anaerobic reactions, the intensity of the monoadduct band was increased, while the aerobic damage at A2 and A3 was accordingly reduced (lanes 13 and 14). Noteworthy in lanes 13 and 14 is the finding of a new set of damage products with the slowest electrophoretical mobility, identical to that found in lanes 5 and 6. These products (indicated by the square bracket) have properties consistent with their representing interstrand cross-links. The bands (arrow) moving more slowly than the intact D1 and faster than the cross-links in lanes 5 and 6 are likely drug monoadducts formed on the oligomer D1 under anaerobic reaction conditions. By using oligomers of different lengths, the two sets of slowly moving bands have been conclusively identified as interstrand cross-links and drug monoadducts (*2*). The minor bands in the cross-linked region are probably caused by incomplete denaturation of the cross-linked DNA under this condition and/or structurally different interstrand cross-links. Strand break and abasic lesions, which are produced in aerobic reactions, are still produced, although at much lesser amounts, under the above described anaerobic reactions. Likely, this was due to residual or contaminating oxygen associated with the prolonged incubation time (3 h or overnight). The remaining "phosphoglycolate" band clearly indicates that some residual oxygen is present.

Quantitation of the damage products showed that the aerobic cleavages at the three sites were reduced by different degrees, when O_2 was depleted from the reactions (data not shown). The amount of aerobic damage at A2, where C1′ hydrogen is abstracted, was markedly reduced, and the cleavage at A3 due to C5′ chemistry was least affected. It is noteworthy that the cleavage at A3 also involves some C4′ chemistry as shown by the typical "phosphoglycolate" band (lane 11, indicated by an arrow). In contrast to the aerobic cleavage by C5′ chemistry at the same site, the "phosphoglycolate" bands almost completely disappeared upon O_2 removal (compare A3 sites in lanes 11 and 12 with lanes 13 and 14). These data demonstrate that the accessibility of O_2 and/or proximity of the drug to the DNA radicals in the drug/DNA complex determine the pathway which leads to different final DNA damage products.

Trapping of DNA Sugar Radicals with Misonidazole. The nitroaromatic radiosensitizer misonidazole has been shown to function efficiently in trapping deoxyribose radicals

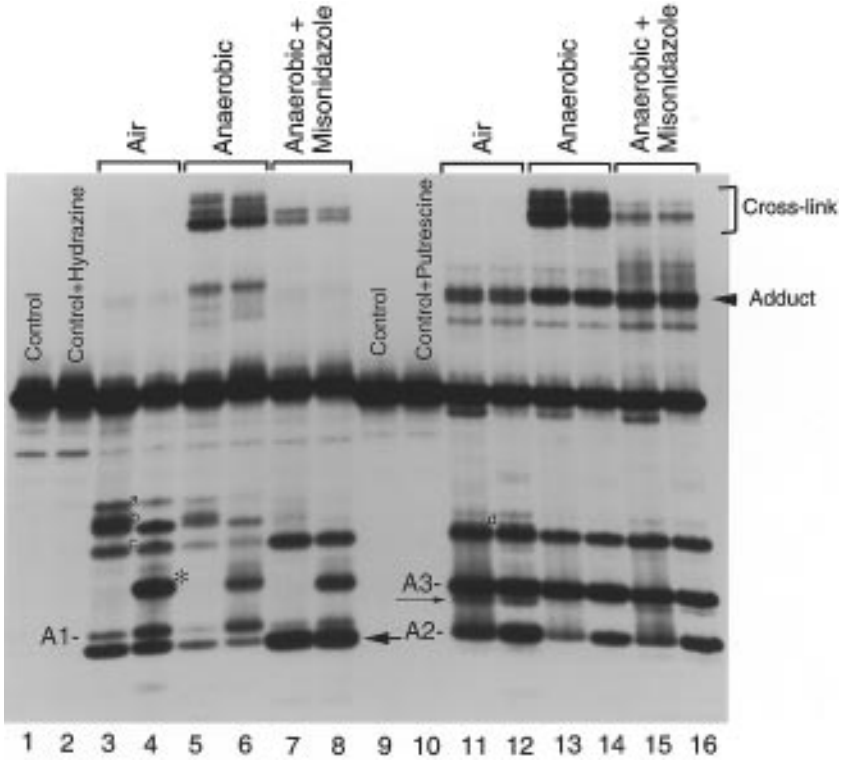

FIGURE 5: Denaturing gel analysis of DNA damage products by C1027. The ^{32}P 5′-end-labeled D1 was annealed to D2 (lanes 1−8) and the 5′-^{32}P end-labeled D2 was annealed to D1 (lanes 9−16). The DNA substrates were incubated for 3 h with C1027 as described in Materials and Methods. Lanes 3, 4, 11, and 12 are samples from aerobic reactions and lanes 5−8 and 13−16 are from anaerobiosis with or without misonidazole. Hydrazine (lanes 2, 4, 6, and 8) and putrescine (lanes 10, 12, 14, and 16) were used to express the abasic lesions at A1 and A2, respectively. The DNA fragments with 3′-phosphoglycolate ends at A1 and A3 sites are indicated by arrows in lanes 3−8 and 11−16, respectively. Asterisk identifies the pyridazine adduct formed by hydrazine treatment.

generated by neocarzinostatin and to thus substitute for O_2 in effecting strand scission (Kappen & Goldberg, 1984). Therefore, it was of interest to use misonidazole as a probe to test the proposal that similar to that in aerobic reaction, the anaerobic reaction process involves hydrogen abstractions. As shown in Figure 5, addition of misonidazole to the anaerobic reactions (lanes 7 and 8) dramatically restores all DNA cleavage products at A1 with the "phosphoglycolate" band (indicated by arrow in lanes 7 and 8) stronger than that in aerobic reaction (compare lanes 7 and 8 with lanes 3 and 4), as noted earlier (*13*). The results are consistent with the proposal that the initiation of anaerobic damage shares the same mechanism with that of aerobic cleavage, i.e., position-specific hydrogens are abstracted by the diradical of the drug. Misonidazole partially restores the aerobic cleavage at A2 sites on the bottom strand. Thus it appears that misonidazole can substitute for O_2 in trapping deoxyribose radicals generated by C1027. Of interest is the finding that whereas monoadduct (and interstrand cross-link) formation involving the top strand is markedly inhibited by inclusion of misonidazole in the anaerobic reaction, monoadduct formation on the bottom strand is insensitive to this agent. It is clear that misonidazole diverts monoadduct formation on the top strand mainly to strand breakage with 3′-phosphoglycolate ends. By contrast, misonidazole (or anaerobiosis) has little influence on strand breakage at A3. The small effect of misonidazole on both cleavage at A3 and monoadduct formation suggests that the monoadduct does involve A3 to a large extent. Cross-link formation involving the bottom strand, however, is strongly inhibited by misonidazole, presumably due to the inhibition of adduct formation on the top strand. It is interesting that neither anaerobiosis nor misonidazole significantly affects either cleavage at A3 or monoadduct formation on the bottom strand, suggesting that sufficient dioxygen is present for this former lesion and that neither dioxygen nor misonidazole is able to compete with the bound drug for putative addition to the carbon-centered deoxyribose radical. It seems that dioxygen is not required for the 5′ chemistry at A3. It is possible that cleavage occurs by a different chemistry, possibly by α-fragmentation at the phosphorus.

Formation of Cross-Links and Monoadducts Involves Position-Specific Hydrogen Abstraction. To test the proposal that the formation of interstrand cross-linking and monoadducts involves position-specific hydrogen abstraction, a hairpin oligo D3 (Figure 3) was synthesized in which deuterium was substituted for the C1′ hydrogen of A2 and ^{32}P 3′-end-labeled. As described above, a single binding mode of C1027 in the 5′GTTA1T/5′ATA2A3C sequence enables the drug diradical to generate two types of DS DNA lesions involving either A1 and A2 or A1 and A3. Because almost all of the damage at the three sites is due to DS cleavage (*11*), there is no apparent cleavage band associated with the A1 site in the hairpin DNA (Figure 6). It has been previously shown that substitution of deuterium at C1′ and A2 results in a substantial isotope selection effect on cleavage at A2 and shuttling of the attack from the C1′ of A2 to the C5′ of the neighboring nucleotide A3 (*9*). As shown in Figure 6, the almost complete loss of damage at A2, due to the remarkable isotope effect ($k_H/k_D = 7.8$) (compare lanes 2 and 3 with 7 and 8), resulted in the shift of attack to A3 (quantitation by PhosphorImager showed that ca. 31% of the

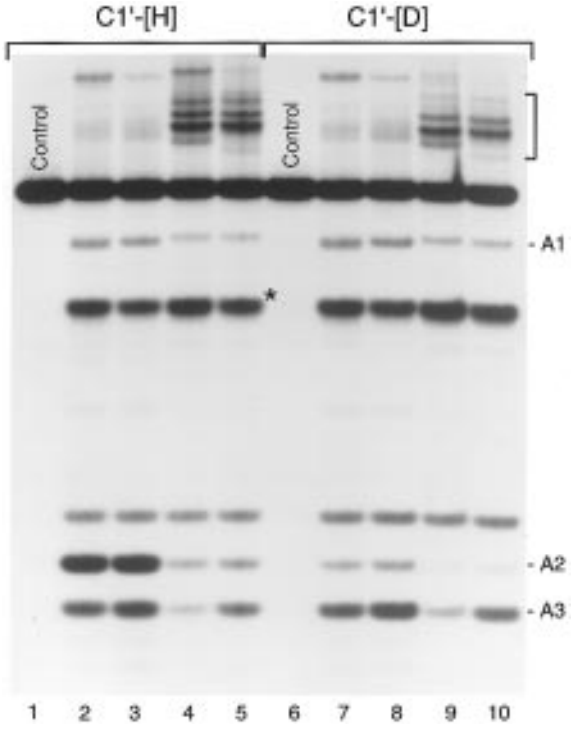

FIGURE 6: Deuterium isotope effect on DNA damage by C1027. ^{32}P 3′-end-labeled D3 was treated with C1027 and then analyzed in a denaturing gel. Lanes 1−5, A2 has C1′-^{1}H; lanes 6−10, A2 site has C1′-^{2}H; lanes 2, 3, 7, and 8, aerobiosis; lanes 4, 5, 9, and 10, anaerobiosis. Lanes 3, 5, 8, and 10 are samples treated with putrescine. The 5′-nucleoside aldehyde bands associated with the A3 site were marked by an asterisk. The possible interstrand cross-links are indicated by a square bracket, and the drug monoadducts are shown by an arrow.

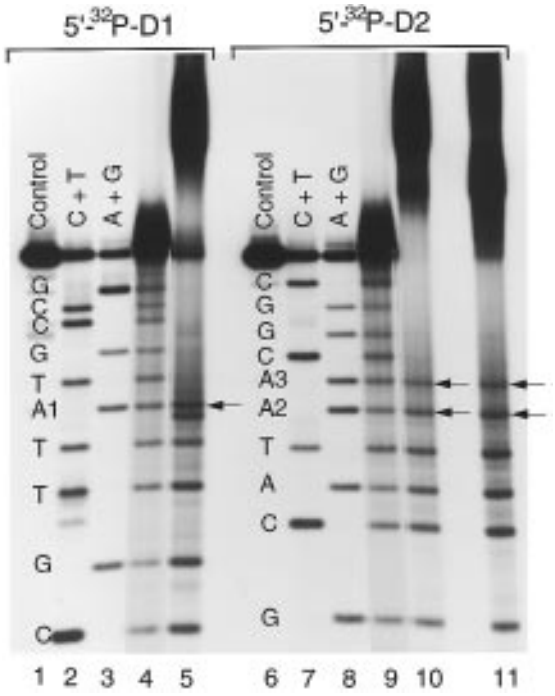

FIGURE 7: Sequence random fragmenation of isolated major DNA cross-links and drug monoadduct. The major DNA cross-link and monoadduct were isolated from preparative gels similar to Figure 5 and subjected to treatment with iron(II) EDTA/ascorbic acid/H_2O_2. Lanes 1 and 6, DNA only; lanes 2, 3, 7, and 8, sequence markers. The other lanes are samples treated with hydroxyl free radicals. Lanes 4 and 9, intact DNA strands; lanes 5 and 10, cross-linked DNA, and lane 11, strand D2 with a drug monoadduct. Cleavage bands, corresponding to Maxam−Gilbert markers, are found only at sites 5′ to the site of adduction or cross-linkage. Fragments of the 3′ side of the adduct or cross-link move more slowly than the starting DNA (see control). The nucleotides where drug attaches are indicated by arrows.

loss of damage at A2 was shifted to A3; compare the 5′-nucleoside aldehyde bands denoted by the asterisk and the cleavage bands associated with A3 in lanes 7−10 with lanes 2−5). The damage at A1 was almost unchanged, which indicates that only hydrogen abstraction by the radical center of the drug diradical responsible for the attack at either A2 or A3 was affected, while the attack by the other radical center was not altered.

Unlike the electrophoretic behaviors of the cross-links and monoadducts associated with the DNA duplexed by complementary single strands, the cross-linked material formed in hairpin D3 (marked by a square bracket) moves slightly faster than the monoadducts, possibly due to incomplete denaturation of the hairpin oligo (data not shown). Of interest is the observation that the overall isotope selection effect on C1027-mediated anaerobic DNA damage by the C1′ deuterium substitution at A2 (k_H/k_D) is 1.8, less than the isotope effect on aerobic cleavage at A2. This suggests that much of the cross-linkage involves A1 and A3. One of the bands, the slowest of the main three interstrand cross-linked materials, however, disappears in the deuterium experiment, showing that it is due to cross-linkage between A1 and A2.

This experiment provides conclusive proof that the formation of cross-links and monoadducts truly involves position-specific hydrogen abstraction. In another separate experiment, DNA was incubated with postactivated C1027 chromophore under similar reaction conditions, but no DNA damage of any kind, including adduct formation, was detected. Therefore, only the diradical of the drug, not the benzoxazolinate or other moieties, initiates the cross-linking and adduction processes in the described C1027/DNA anaerobic reactions.

Nucleotide Connectivities of Cross-Links and Monoadducts. The nucleotide connectivities of the interstrand cross-linked DNA and the drug monoadduct on D2 of duplex D1 plus D2 were determined by sequence-random cleavage with iron(II) EDTA/ascorbic acid/hydrogen peroxide (*10*). The major band with least electrophoretic mobility, representing cross-linked DNA, and the slow D2 drug monoadduct band were isolated from the denaturing gel. The sites of cross-linking and adduction were identified at nucleotide resolution by sequence random oxidative fragmentation followed by high-resolution sequencing gel analysis of the oligomer fragment mixture. As shown in Figure 7, in the resulting ladder of 5′-[^{32}P]D1 fragments shorter in length than the starting single strand is the absence of fragments derived from cleavage at the non-radiolabeled, 3′-side of the A1 residue (compare lane 5 with lane 4). On the complementary strand, D2, the distribution of fragments randomly generated from the cross-linked strands and drug monoadducts stopped at the A3 residue (compare lanes 10 and 11 with lane 9). However, the intensities of the bands corresponding to A3 in lanes 10 and 11 are somewhat weaker than those of the bands comigrating with A2, consistent with, but not proof of, the presence of adduct at A2. These results support the A1 to A3 or A1 to A2 connectivities of the interstrand cross-links and the attachment of the monoadducts on either A3 or A2 at the 5′GTTA1T/5′ATA2A3C sequence. Further, the

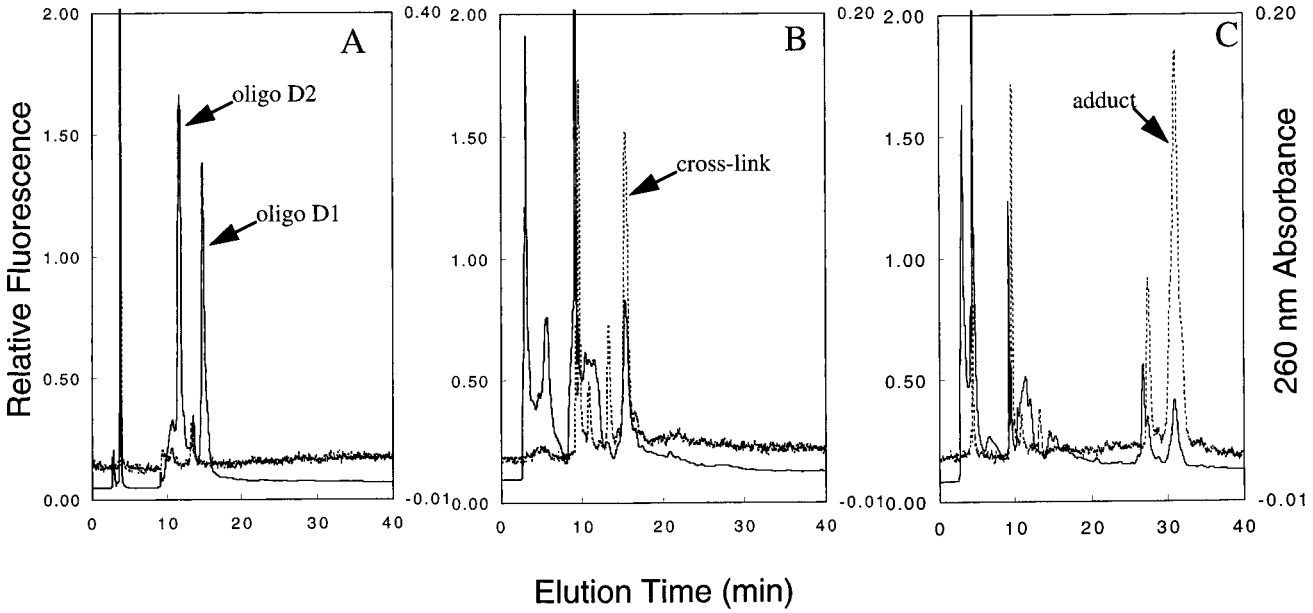

FIGURE 8: HPLC profile of C1027-induced DNA damage products under anaerobiosis. Solid and broken lines are 260 nm UV absorbance and 435 nm fluorescence excited at 350 nm, respectively. (A) Duplex D1:D2; (B) cross-linked material from gel; (C) drug monoadduct from gel. Samples for HPLC were prepared as described in Materials and Methods.

binding of C1027 to DNA is covalent. The new band with slowest mobility in lane 11 may be caused by interstrand cross-linking during the oxidative fragmentation.

HPLC Separation of Anaerobic Damage Products by C1027. The anaerobic damage products were purified in two steps. Firstly, samples were separated by high-resolution denaturing gels. Duplexed DNA oligos, interstrand cross-links, and drug monoadducts were thus separated and visualized with UV shadowing. The bands containing major cross-links and drug monoadducts were excised and eluted by shaking overnight. The supernatants containing cross-links and drug adducts were then subjected to reverse-phase HPLC purification on a C-18 column using a solvent gradient as described in Materials and Methods. Under the described elution conditions, duplex D1:D2 is well denatured and the two strands are separated, as detected at 15 and 11 min, respectively (Figure 8A). The sample corresponding to the major cross-linking band is eluted at about 16 min, as detected by both 260 nm UV absorbance and 435 nm fluorescence (excited at 350 nm) (Figure 8B). The drug adduct eluted at 31 min with a much stronger fluorescence (Figure 8C). The HPLC experiments provided further evidence that two different kinds of anaerobic DNA damage products are formed, which involve the covalent binding of drug onto DNA. The UV absorbance peaks and some fluorescence peaks between 3 and 14 min (B and C) are probably substances from the denaturing gel or decomposed products from the cross-links and monoadducts. The results of mass spectrometry studies are consistent with the theoretical masses of the interstrand cross-link (Figure 8B) and drug monoadduct (Figure 8C) (*2*). Additional structural studies with these HPLC purified samples are in progress.

Anaerobic Damage Induced by Calicheamicin γ_1^I. The experimental results described above suggest that when the DNA deoxyribose radicals, formed by the attack of drug diradical, could not be oxidized or trapped by other hydrogen sources, they reacted covalently instead with the bound drug in near proximity to form minor groove-based drug monoadducts or interstrand cross-links. To provide further evidence, other enediyne/DNA reaction systems were explored under similar conditions.

It has been demonstrated that calicheamicin γ_1^I cleaves DNA sequence-specifically with predominantly DS lesion (*15*). Tetranucleotide pyrimidine tracts, such as TCCT and CTCT, were found to be prominent binding/cleaving sites (*16*). Studies with DNA containing the 5′TC1CT/5′AGGATC2 site indicated that the DS lesions are staggered by three nucleotides to the 3′-side of the cleavage site. The C5′ of C1 is attacked by the C6 radical of the 3,6-diradical of the drug (Figure 1) to give a strand break due to C5′-chemistry (Figure 9, lane 3). The C4′-hydrogen abstraction by the C3 radical of the drug results in 3′-phosphoglycolate and an abasic lesion due to C4′ chemistry (lane 6) (*15*). Depletion of O_2 reduced the amount of aerobic cleavage at both C1 and C2 sites, and two new sets of slowly moving bands were generated (lanes 5 and 8). It is interesting that calicheamicin γ_1^I mainly produces drug monoadducts, which are mostly formed on bottom strand D11, not interstrand cross-links. The method for distinguishing monoadducts and interstrand cross-links is the same as previously reported (*2*). Another interesting observation is that unlike the cleavage at A3 induced by C1027 due to C5′ hydrogen abstraction (Figure 5, lanes 14 and 15), the damage at C1 was dramatically reduced, but interestingly only a small amount of adduct is generated on this strand (compare lane 3 with lane 4 and lane 4 with lane 8). Position-specific quenching of this DNA radical by solvent and/or thiol might explain this observation.

Anaerobic Damage Induced by Neocarzinostatin. Like C1027, neocarzinostatin, when activated by thiols, can produce sequence-specific DS lesions at 5′AGC1/5′GCT2 and 5′AGT1/5′ACT2 sites (*17*, *18*). Aerobic DS lesions at the 5′AGC1/5′GCT2 site consists of an apyrimidine site at C1 due to 2′-deoxyribonolactone formation (C1′ chemistry) and a break resulting from 3′-PO_4 formation (C5′ chemistry) (Figure 10, lanes 2 and 5) (*18*). At the 5′AGT1/5′ACT2 site, strand breaks at T2 (C5′ chemistry) and T1 (C4′ chemistry) and an abasic lesion at T2 (C4′ chemistry) are

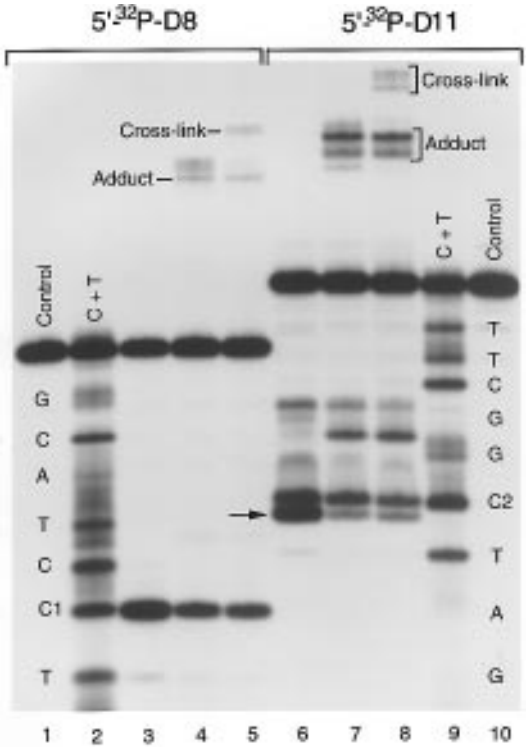

FIGURE 9: Denaturing gel analysis of DNA damage products by calicheamicin γ_1^I at room temperature overnight. 5′-End-labeled D8 was annealed to D9 (lanes 3 and 4) and D11 (lane 5), and the 5′-end-labeled D11 was annealed to D8 (lanes 6 and 7) and D10 (lane 8). Calicheamicin γ_1^I was added in methanol (5%) was incubated with DNA in the presence of 1 mM glutathione under similar conditions as described in Figure 5. Samples in lanes 3 and 6 are from aerobic reactions and lanes, 4, 5, 7, and 8 are samples from anaerobiosis. The two sets of slow moving bands were denoted by adduct and cross-link. The damage at C1 generates strand breaks due to C5′ chemistry. The arrow indicates the "phosphoglycolate" band due to C4′ chemistry at C2 sites.

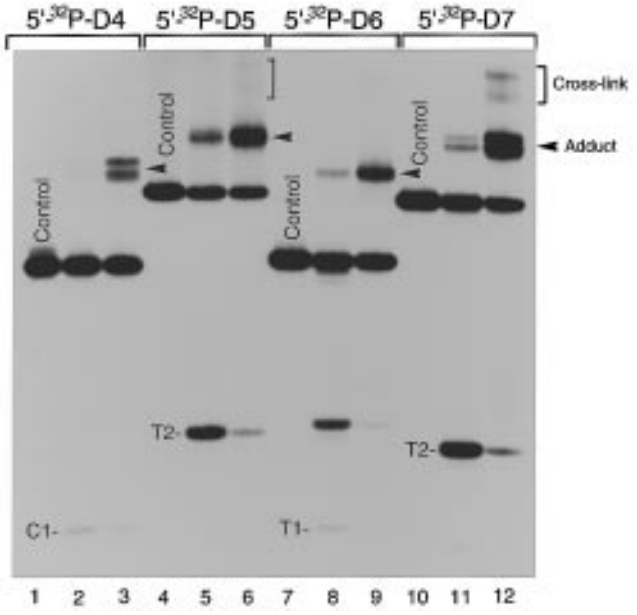

FIGURE 10: Gel analysis of DNA damage products by neocarzinostatin at the 5′AGC1/5′GCT2 and 5′AGT1/5′ACT2 sites in the presence of 1 mM DTT. Reactions were carried out in dark at room temperature overnight. Lanes 1−3, 5′-[^{32}P]D4 annealed to D5; lanes 4−6, 5′-[^{32}P]D5 annealed to D4; lanes 7−9, 5′-[^{32}P]D6 annealed to D7; and lanes 10−12, 5′-[^{32}P]D7 annealed to D6. Samples in lanes, 2, 5, 8, and 11 are from aerobic reactions, and those in lanes 3, 6, 9, and 12 are from anearobiosis. The DS damage sites are denoted by C1 (lane 2), T2 (lanes 5 and 11), and T1 (lane 8).

generated (Figure 10, lanes 8 and 11) (*17*). Under anaerobic conditions, almost all the bands moving slower than starting DNA generated by neocarzinostatin are drug monoadducts (lanes 3, 6, 9, and 12), which are identified by using oligomers of different lengths, as reported (*2*). It is interesting to note that unlike in C1027/DNA reactions, the aerobic damage at the two T2 sites, where C5′-hydrogens are abstracted, is dramatically reduced by the O_2 depletion (compare A3 sites in lane 14 with 16 in Figure 5 and T2 sites in lane 5 with 6 and in lane 11 with 12 in Figure 10) similar to the calicheamicin/DNA reaction. In another experiment with glutathione as the drug activator, it was found that there was much less adduct and cross-link formation (data not shown). Taken together, it is clearly demonstrated that strand breakage resulting from C5′-hydrogen abstraction requires molecular oxygen and the accessibility and/or proximity of the drug, hydrogen sources, and O_2 to the deoxyribose radicals play an important role in determination of the fate of the radicals and the types of resulting damage products.

DISCUSSION

Enediyne antitumor antibiotics, when activated either by thiols or in a spontaneous process, cycloaromatize through a Bergman-type reaction to generate a reactive biradical species (*1*, *19*). If properly positioned inside the minor groove of duplex DNA, the biradical species can abstract hydrogen atoms from deoxyriboses of one or both complementary strands of duplex DNA. In the presence of O_2, the DNA sugar radicals thus generated are oxidized, resulting ultimately in oxidative SS or DS DNA lesions including strand breaks and abasic sites. Proper positioning of the drug biradical, which also determines the ratio of SS/DS lesions, depends on the interaction between specific drug molecules with the DNA microstructure (sequence determined), mainly by intercalation and/or hydrophobic interactions in the DNA minor groove (*20*, *21*). Under anaerobic conditions, the newly generated deoxyribosyl radical of each complementary DNA strand likely reacts covalently with the bound drug to form minor-groove-based interstrand cross-links or drug monoadducts. The success rate of the biradical drug in generating interstrand cross-links and monoadducts and the ratio of interstrand cross-links (involving both strands) and monoadducts (involving only one strand) appears to vary from drug to drug. The factors, which determine whether and how anaerobic damage products are generated, are discussed below.

Position-Specific Hydrogen Abstraction. It is well established that the aerobic damage induced by enediynes involves hydrogen abstraction from deoxyribose (*22*). Activation of neocarzinostatin to its radical species and hydrogen atom abstraction from the C5′ position, however, occur normally under anaerobic conditions (*23*). To exclude the possibility that other moieties of the drugs, such as the benzoxazolinate moiety of C1027, might be involved in the reactions, identical drug/DNA reactions were done with postactivated C1027 chromophore, and no evidence of adduct formation was obtained. Conclusive proof for hydrogen abstraction, initiating the interstrand cross-linking and adducting comes from the observed isotope effects by deuterium substitution of C1′-

hydrogen at A2 of 5′GTTA1T/5′ATA2A3C sequence in the C1027/DNA reaction system.

The ratio of interstrand cross-links/monoadducts seems to vary from drug to drug because the success rate of each radical center of the drug biradical in hydrogen abstraction from deoxyribose and the proximity of the drug to the deoxyribose radicals are not necessarily equal. In the case of neocarzinostatin, one radical center (C6 of the 2,6-diradical) (Figure 1) is highly efficient in hydrogen abstraction from the T2 residue in 5′AGC1/GCT2 or 5′AGT1/5′ACT2, whereas the other radical center (C2 of the 2,6-diradical) is somewhat less so in hydrogen abstraction from C1 or T1 residues on the complementary strands. This results in a substantial number of SS lesions and hence a predominant amount of monoadducts on oligo D5 or D7 (compare lanes 2 and 3 with lanes 5 and 6 and lanes 8 and 9 with lanes 11 and 12 in Figure 10). The C2 radical center of neocarzinostatin was found to be more exposed in the activated drug/DNA complex and is readily quenched by solvent (*24*, *25*). Similarly, it has been reported that one of the radical centers of activated C1027, responsible for attacking either A2 or A3 in the target 5′GTTA1T/5′ATA2A3C sequence, is more exposed, and only this radical or its consequent deoxyribosyl radical can be quenched by solvent methanol (*9*). Without methanol, both radical centers are equally efficient in hydrogen abstraction from deoxyribose, and consequent oxidative deoxyribose damage and almost all damage in this sequence is in the form of DS lesions. Thus, C1027 produces much more interstrand cross-links than neocarzinostatin under similar anaerobic reactions. Consistent with an earlier report (*15*), Figure 9 shows that calicheamicin γ_1^I induces mainly DS lesions. However, calicheamicin γ_1^I produces much less interstrand cross-linkage and drug monoadduct formation than C1027 or neocarzinostatin under similar anaerobic conditions, implicating other geometrical influences.

Radical Quenchers in the Reaction Mixture. As described above, solvent methanol may selectively quench one of the biradical centers of the neocarzinostatin or C1027 chromophore. In the same manner, the hydrogen sources in the reaction mixture, such as methanol or thiols, can also quench the DNA radicals formed by the bifunctional drug, although both of the biradical centers can escape quenching by solvent and efficiently abstract hydrogens from the complementary DNA strands. As evidence of the accessibility of radical quenchers to DNA radicals, misonidazole, an aromatic radiosensitizer, was shown to be a successful DNA radical trapper, which restores the cleavage reactions under anaerobic conditions involving C1027 (Figure 5) or neocarzinostatin (*13*). Recently, evidence for selective deoxyribosyl radical repair by thiol in the case of the enediyne esperamicin A has been reported (*26*). In another experiment with neocarzinostatin, glutathione was added as the drug activator and there was much less interstrand cross-links and fewer drug monoadducts were generated (data not shown). In the calicheamicin/DNA reaction system, glutathione and methanol were added as the drug activator and carrier, respectively. It is possible that either glutathione or methanol quenches the DNA radicals, resulting in production of fewer interstrand cross-links and monoadducts.

Proximity of Drug to DNA Radical. As has been demonstrated earlier, the distance between the drug radical and the position-specific hydrogen of deoxyribose determines the efficiency of hydrogen abstraction (*20*). Proximity of the postactivated drug to the DNA radical should also be an important factor in the efficient production of interstrand cross-links and drug monoadducts. As in hydrogen abstraction, the proximity of drug to the DNA radical should be dependent on the specific postactivated drug/DNA interaction, which varies from drug to drug. It is also possible that different efficiencies in production of interstrand cross-links and monoadducts in different drug/DNA reaction systems under similar anaerobic conditions result from different drug/DNA interactions or proximity of drug to DNA radicals.

In conclusion, enediyne antibiotics bind to duplex DNA in a sequence-selective manner, which positions the enediyne cores in the minor groove. When activated, the bifunctional drug can position-specifically abstract the nearest hydrogens from deoxyribose of DNA backbones. The newly formed DNA sugar radical can be oxidized to generate abasic sites and strand breaks. Without O_2, however, the DNA radical is able to add back onto the nearby unsaturated system of the postactivated enediyne core. This process is a kinetically competitive one, depending on the proximity of the drug-unsaturated system to the sugar radical and the quenching by O_2 or other hydrogen sources such as solvent or thiols. C1027 mainly induces interstrand cross-links, whereas most of the anaerobic lesions produced by neocarzinostatin are monoadducts. Calicheamicin γ_1^I is found to be less efficient in generating either interstrand cross-links or monoadducts.

REFERENCES

1. Goldberg, I. H., Kappen, L. S., Xu, Y. J., Stassinopoulos, A., Zeng, X., Xi, Z., and Yang, C. F. (1996) in *DNA and RNA Cleavers and Chemotherapy of Cancer and Viral Diseases* (Meunier, B. Ed.) NATO Advanced Science Institute Series, Series C, pp 1−21, Kluwer Academic Publishers, Dordrecht, The Netherlands.
2. Xu, Y. J., Zhen, Y. S., and Goldberg, I. H. (1997) *J. Am. Chem. Soc. 119*, 1133−1134.
3. Povirk, L. F., and Goldberg, I. H. (1982) *Proc. Natl. Acad. Sci. U.S.A. 79*, 369−373.
4. Povirk, L. F., and Goldberg, I. H. (1982) *Nucleic Acids Res. 10*, 6255−6264.
5. Povirk, L. F., and Goldberg, I. H. (1984) *Biochemistry 23*, 6304−6311.
6. Hu, J. L., Xue, Y. C., Xie, M. Y., Zhang, R., Otani, T., Minami, Y., Yamada, Y., and Marunaka, T. (1988) *J. Antibiot. 41*, 1575−1579.
7. Otani, T., Minami, Y.; Marunaka, T., Zhang, R., and Xie, M. (1988) *J. Antibiot. 41*, 1580−1585.
8. Zhen, Y. S., Ming, X. Y., Yu, B., Otani, T., Saito, H., and Yamada, Y. (1989) *J. Antibiot. 42*, 1294−1298.
9. Xu, Y. J., Xi, Z., Zhen, Y. S., and Goldberg, I. H. (1995) *Biochemistry 34*, 12451−12460.
10. Tullius, T. D., and Dombroski, B. A. (1985) *Science 230*, 679−681.
11. Yu, L., Mah, S., Otani, T., and Dedon, P. (1995) *J. Am. Chem. Soc. 117*, 8877−8878.
12. Xu, Y. J., Zhen, Y. S., and Goldberg, I. H. (1994) *Biochemistry 33*, 5947−5954.
13. Kappen, L. S., Goldberg, I. H., Frank, B. L., Worth, L., Jr., Christner, D. F., Kozarich, J. W., and Stubbe, J. (1991) *Biochemistry 30*, 2034−2042.
14. Kappen, L. S., and Goldberg, I. H. (1984) *Proc. Natl. Acad. Sci. U.S.A. 81*, 3312−3316.
15. Dedon, P. C., Salzberg, A. A., and Xu, J. (1993) *Biochemistry 32*, 3617−3622.
16. Zein, N., Sinha, A. M., McGahren, W. J., and Ellestad, G. A. (1988) *Science*, *240*, 1198−1201.
17. Dedon, P. C., and Goldberg, I. H. (1990) *J. Biol. Chem. 265*, 14713−14716.

18. Povirk, L. F., Houlgrave, C. W., and Han, Y. H. (1988) *J. Biol. Chem. 263*, 19263−19266.
19. Nicoloau, K. C., Dai, W. M., Tsay, S. C., Estevez, V. A., and Wrasidlo, W. (1992) *Science 256*, 1172−1178.
20. Gao, X., Stassinopoulos, A., Rice, J. S., and Goldberg, I. H. (1995) *Biochemistry 34*, 40−49.
21. Kappen, L. S., and Goldberg, I. H. (1992) *Proc. Natl. Acad. Sci. U.S.A. 89*, 6706−6710.
22. Xi, Z., and Goldberg, I. H., in *Comprehensive Natural Products Chemistry* (Barton, D. H., and Nakanishi, K., Eds.) Elsevier Science, Oxford, in press.
23. Kappen, L. S., and Goldberg, I. H. (1985) *Nucleic Acids Res. 13*, 1637−1648.
24. Meschwitz, S. M., Schultz, R. G., Ashley, G. W., and Goldberg, I. H. (1992) *Biochemistry 31*, 9117−9121.
25. Chin, D. H., and Goldberg, I. H. (1993) *Biochemistry 32*, 3611−3616.
26. Epstein, J. L., Zhang, X., Doss, G. A., Liesch, J. M., Krishnan, B., Stubbe, J., and Kozarich, J. W. (1997) *J. Am. Chem. Soc. 119*, 6731−6738.

BI972101O